

## Original Article

# Osteogenesis of bone marrow mesenchymal stem cells on nano-hydroxyapatite/bacterial cellulose copposite scaffolds in rats

Tong-Qu Song<sup>1</sup>, Bao-Jian Ge<sup>2</sup>, Hung-Liang Chen<sup>2</sup>, Xiao-Wei Yang<sup>3</sup>, Feng Yuan<sup>2</sup>

<sup>1</sup>Department of Spinal Surgery, Xuzhou Central Hospital, Xuzhou 221000, Jiangsu, China; <sup>2</sup>Department of Spinal Surgery, The Affiliated Hospital of Xuzhou Medical University, Xuzhou 221000, Jiangsu, China; <sup>3</sup>Department of Spinal Surgery, The Third People's Hospital of Xuzhou, Xuzhou 221000, Jiangsu, China

Received June 24, 2016; Accepted August 30, 2016; Epub October 1, 2016; Published October 15, 2016

**Abstract:** The composite scaffolds are extensively employed to repair and reconstruct damaged bone tissue function. The present study was designed to explore the nano-hydroxyapatite/bacterial cellulose (nHA/BC) on the proliferation and osteogenic differentiation of rat bone marrow mesenchymal stem cells (BMSCs). The osteoblast induced BMSCs were cultured on nHA/BC scaffolds. The proliferation of BMSCs was determined by the cell counting kit-8 (CCK-8) assay. The osteogenic response of BMSCs to nHA/BC scaffolds was examined by alizarin red staining. The mice were divided into three groups: BMSCs +  $\beta$ nHA/BC, osteoblastic BMSCs + nHA/BC and nHA/BC without cells. The scaffolds of nHA/BC exhibited a good compatibility to BMSCs, and significantly promoted the proliferation of BMSCs, and obviously improved calcium deposition. The osteoblastic BMSCs on nHA/BC scaffolds stimulated the phosphorylation of p38. In addition, the recombination of osteoblastic BMSCs with nHA/BC composite significantly boosted the bone formation *in vivo*. The scaffolds of nHA/BC may enhance the proliferation and osteoblastic differentiation of BMSCs via modulation of p38 signal transduction pathway. The recombination of nHA/BC scaffolds with BMSCs exerts good ability of ectopic osteoblast, and they may be served as a kind of bone substitute for bone regeneration.

**Keywords:** Osteogenesis, bone mesenchymal stem cells, nHA/BC

## Introduction

The goal of bone tissue engineering is to replace defect area or damaged tissue by implanting bone substitutes [1, 2]. Bone tissue engineering emerges as a promising way for bone regeneration to recover the body's normal physiological structure and function [3]. Seed cells, growth factors and scaffolds are essential components during produces for bone tissue engineering [4]. Numerous investigations have confirmed the feasibility of composite scaffolds for bone tissue engineering [5]. Tissue engineered scaffolds are widely used to repair and reconstruct damaged bone tissue function [6]. The weight ratio of compound, pore size, porosity and mechanical properties are crucial factors for influencing clinical application of the composite scaffolds [7].

Bone marrow-derived mesenchymal stem cells (BMSCs) are recognized as a valuable cell type

for bone regeneration, and are widely used in cytotherapy for musculoskeletal diseases [8]. BMSCs are usually considered as seed cells in cytotherapy due to their differentiation ability into osteogenic and chondrogenic lineages [8, 9]. Furthermore, BMSCs are extensively used for tissue engineering for their low immunogenicity, abundant material source and multi-directional differentiation potency [10]. To date, the approaches based on the seeding of BMSCs into biodegradable polymeric scaffolds have been greatly developed by many researchers [11]. Previous study showed that the composite scaffolds of poly ( $\epsilon$ -caprolactone), thermoplastic zein and hydroxyapatite (PCL/TZ-HA) significantly promoted the proliferation and osteogenic differentiation of rabbit BMCSs *in vitro* [12]. Another study proved that BMSCs on hydroxyapatite scaffolds exhibited a faster and better healing of bone segmental defects [13]. Nano-hydroxyapatite (nHA) is demonstrated to a ho-

peful biomaterial for bone repair due to its bioactivity, biocompatibility and osteoconductivity [14].

Bacterial cellulose (BC) is also used for bone tissue regeneration in tissue engineering, due to its high biocompatibility, high crystallinity, high tensile strength and elastic modulus, and good biodegradability [15]. However, it is still unclear whether nHA/BC composite scaffolds could have excellent bioactivity of attachment, proliferation and osteoblastic differentiation for BMSCs. The present study was designed to investigate the role of nHA/BC composite scaffolds on the proliferation, osteogenic differentiation and osteogenesis of rat BMSCs *in vitro* and *in vivo*.

### Materials and methods

#### Animals

The experiments were conformed to the recommendations in the Guide for the Care and Use of Laboratory Animals of the National Institutes of Health. The procedures were reviewed and approved by the Committee on the Ethics of Animal Experiments of Xuzhou Medical University. The male rats were purchased from Laboratory Animal Center, Xuzhou Medical University and caged in temperature-controlled and humidity-controlled room with a 12 h light and 12 h dark cycle, and were provided standard chow and tap water *ad libitum*.

#### Preparation of scaffolds

The nHA/BC scaffolds were synthesized by a biomimetic technique [16-18] and kindly provided by Material Institute of Tianjing University. Before BMSCs seeding, the nHA/BC scaffolds were pre-wetted in DMEM-F12 medium for 4 h and dried in an incubator overnight under sterile conditions.

#### Isolation and expansion of BMSCs

BMSCs were isolated and cultured as previously described [19]. In brief, the Sprague-Dawley (SD) rats aged 3 months old were sacrificed by an overdose of pentobarbital sodium (150 mg/kg, *iv*). The femurs, muscle and connective tissue of each rat were aseptically excised, and the bone marrow was extracted by flushing the

medullar cavities under sterile conditions. The collected marrow was flushed with essential culture media (DMEM supplemented with 10% FBS, 100 U/ml penicillin, and 100 µg/ml streptomycin) by a 27-gauge needle attached to a 10 ml syringe. The cell suspension was centrifuged at 1000 rpm for 10 min, and then the whole cells were re-suspended in fresh primary media and added into Percoll separating medium (GIBCOBRL company), and were seeded into a 25 cm<sup>2</sup> flask for incubation in a 5% CO<sub>2</sub> incubator at 37°C with 95% humidity. The non-adherent cells were washed away after 48 h by replacing the medium with fresh complete medium. Then the medium was exchanged every three days and the cells were passaged when the cells grew on reaching a confluence of 80-90% in the flasks.

#### Flow cytometry

BMSCs were characterized and confirmed by analysis of cell surface markers (CD29, CD34, CD44 and CD90) with flow cytometry as previous report [20]. BMSCs at passage 3 were incubated with 0.25% trypsin-EDTA (ethylene diamine tetraacetic acid) for 2 min at 37°C and subjected to centrifugation at 1000 r for 5 min. The obtained cells were washed with phosphate-buffered saline (PBS), and the cells were then subsequently cultured with rat monoclonal anti-CD29-FITC (BD Biosciences, San Jose, CA, USA), rat polyclonal anti-CD34-FITC (Bioss Biosynthesis Biotechnology Co., Ltd., Beijing, China), rat polyclonal anti-CD44-PE (R&D Systems, Inc., Minneapolis, MN, USA), and rat polyclonal anti-CD90-PE (Bioss Biosynthesis Biotechnology Co., Ltd., Beijing, China) for 30 min incubation in the dark at 4°C. The cells were washed by PBS and analyzed using a flow cytometer (Gallios; Beckman Coulter, Brea, CA, USA).

#### Morphology and proliferation of BMSCs on nHA/BC scaffolds

The confluent BMSCs at passage 3 were digested with 0.25% trypsin-EDTA, and seeded onto nHA/BC scaffolds-placed 24 wells with 10<sup>5</sup> cells per ml under a 5% CO<sub>2</sub> incubator at 37°C with 95% humidity. The cells on nHA/BC composite scaffolds were changed with fresh DMEM medium supplemented with 10% FBS after 24 h. Inverted phase contrast microscope was

used to investigate the cellular morphology and attachment of BMSCs on nHA/BC copositive scaffolds [20]. CCK-8 assay was applied to detect the proliferation of the BMSCs on nHA/BC scaffolds [21].

### *Osteogenic induction of BMSCs*

The BMSCs at passage 3 were trypsinized and seeded at a density of  $10^5$ /ml into nHA/BC scaffolds-placed 6 well plates or non-scaffolds-placed 6 well plates and then incubated overnight at 37°C and 5% CO<sub>2</sub> to permit cell attachment. The medium was replaced with osteogenic induction medium after 24 h. The osteogenic induction medium contained  $10^{-7}$  mol/L dexamethasone (Sigma-Aldrich), 10 mmol/L  $\beta$ -glycerophosphate (China Pharmaceutical Shanghai Chemical Reagent Co., Ltd.), 50  $\mu$ g/ml ascorbic acid (Sigma-Aldrich), 1% penicillin/streptomycin and 10% FBS in DMEM [22]. BMSCs were planted on nHA/BC support and cultured by osteogenic induction medium (Group A); BMSCs were cultured by osteogenic induction medium (Group B); BMSCs were planted on nHA/BC support and cultured by DMEM medium (Group C); BMSCs were cultured by DMEM medium (Group D). The calcium nodules deposited in the extracellular matrix of BMSCs in four groups were detected with alizarin red staining after the three-week induction, and the calcium nodule staining was captured by Canon DSLR camera.

### *Western blot*

After induction in osteogenic medium or DMEM medium for one week in four groups, the BMSCs were harvested and were lysed using 100  $\mu$ l of radioimmunoprecipitation assay (RIPA) lysis buffer (Beyotime Institute of Biotechnology, Shanghai, China). The samples were then centrifuged and total protein concentration was measured using the Bicinchoninic Acid kit. Equal quantities of total protein in each group were subjected to sodium dodecyl sulfate polyacrylamide gel electrophoresis and transferred onto polyvinylidene fluoride membrane. The membrane was blocked with 5% non-fat milk for 60 min at room temperature, following by overnight incubation with rabbit anti-p38 (Cell Signaling Technology, Beverly, MA, USA), rabbit anti-phosphorylated p38 (Cell Signaling Tech-

nology, Beverly, MA, USA) and rabbit anti-GAPDH (Santa Cruz, CA, USA) at 4°C. The membrane was incubated with a secondary antibody conjugated to horseradish peroxidase, and visualized by the enhanced chemiluminescent reagent (Merck Millipore, Billerica, Massachusetts, USA). GAPDH was served as an internal control [23].

### *Ectopic bone formation by implantation and degradation test in vivo*

The approval of the surgery of animals was the same with those stated in the isolation section of BMSCs. All rats were anaesthetized with sodium pentobarbital (50 mg/kg, i.p.) and placed in a lateral position. The adequacy of anesthesia was determined by the absence of corneal reflexes and paw withdrawal response to a noxious pinch and surgical manipulation [24]. The rats were divided into three groups: BMSCs +  $\beta$ -nHA/BC, osteoblastic BMSCs + nHA/BC and nHA/BC without cells. After preparation of the skin, a long incision was made along the bilateral back axis, and the muscle was bluntly dissected, and intramuscular pouches including one muscle pouch on the left and two muscle pouch on the right were created in this model. The BMSCs/scaffold composites or scaffolds were implanted into the spatium intermusculare. The left muscle pouch was implanted with osteoblastic BMSCs + nHA/BC scaffolds, the nHA/BC without cells was implanted into upper right side muscle pouch, and BMSCs + nHA/BC were implanted into upper lower side muscle pouch. All the disk scaffolds seeded with  $8 \times 10^5$  cells as previously described. The incisions were sutured and the rats were fed at the condition of cleaned cages with water and food *ad libitum*. The rats were anesthetized at 12 weeks after implantation via intraperitoneal injection with a 10% chloral hydrate solution (0.4 ml/100 g), and were then scanned along the back axial plane by computerized tomography (CT, Light Speed 64 slice spiral CT, General Electric, USA, 2.5 mm slice thickness). The position and bone formation in the implants were observed in the CT images, and the implanting materials were taken out and observed by visual [25]. In addition, the rats were sacrificed and implants with the surrounding tissues were harvested. Paraffin 5  $\mu$ m-thick sections were prepared and stained

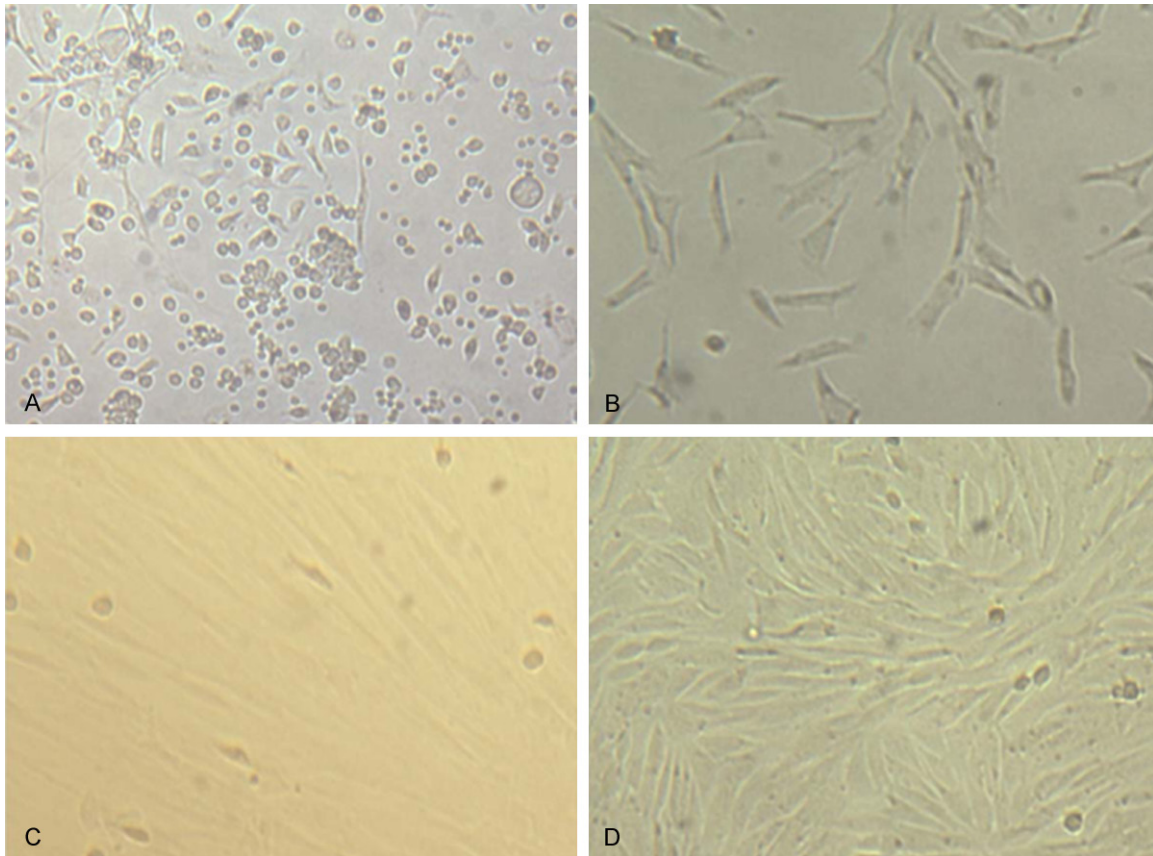


**Figure 1.** Identification of BMSCs in rats. A. The characteristics of primary BMSCs culture after three days. B. The BMSCs at the first passage. C. The BMSCs at the second passage. D. The BMSCs at the third passage. BMSCs, Bone Marrow Mesenchymal Stem Cells.

with hematoxylin and eosin (HE) to observe the ectopic bone formation in rat [26].

## Statistics analysis

All data were expressed as mean  $\pm$  SE. All experiments were repeated at least three times. The statistical analysis was conducted by SPSS 19.0 software (SPSS Inc., Chicago, IL, USA). Comparisons between two groups were made by Student's *t* test. Differences within groups in multiple assays were tested by ANOVA and Dunnett's *t*-test. A value of  $P < 0.05$  was considered statistically significant.

## Results

### Identification of rat BMSCs

The primary BMSCs of rats presented attachment to the wall and characterized as circle or oval shape with strong refraction after 36 h culture. The primary BMSCs showed to be short fusiform, triangular or polygonal shape after three days' culture (**Figure 1A**). The BMSCs

were purified and passaged upon 90% confluence at 14 d, and the BMSCs were uniform long fusiform at the first passage (**Figure 1B**). The BMSCs at the second passage were grown to totally confluence about 5~7 d culture with uniform morphology (**Figure 1C**). The BMSCs at the third passage were in swirling and paralleled growth and presented as long fusiform (**Figure 1D**).

### Detection of surface antigen of rat BMSCs at the third passage with flow cytometry

The surface markers on BMSCs at the third passage were detected with flow cytometry. The immunophenotype of BMSCs was characterized by positive expression of CD29, CD44 and CD90, and negative expression of CD34. Our results showed that the positive rate of CD29, CD44, CD90 were 98.58% (**Figure 2A**), 97.51% (**Figure 2B**), 97.20% (**Figure 2C**), and the negative rate of CD34 was 94.22% (**Figure 2D**).



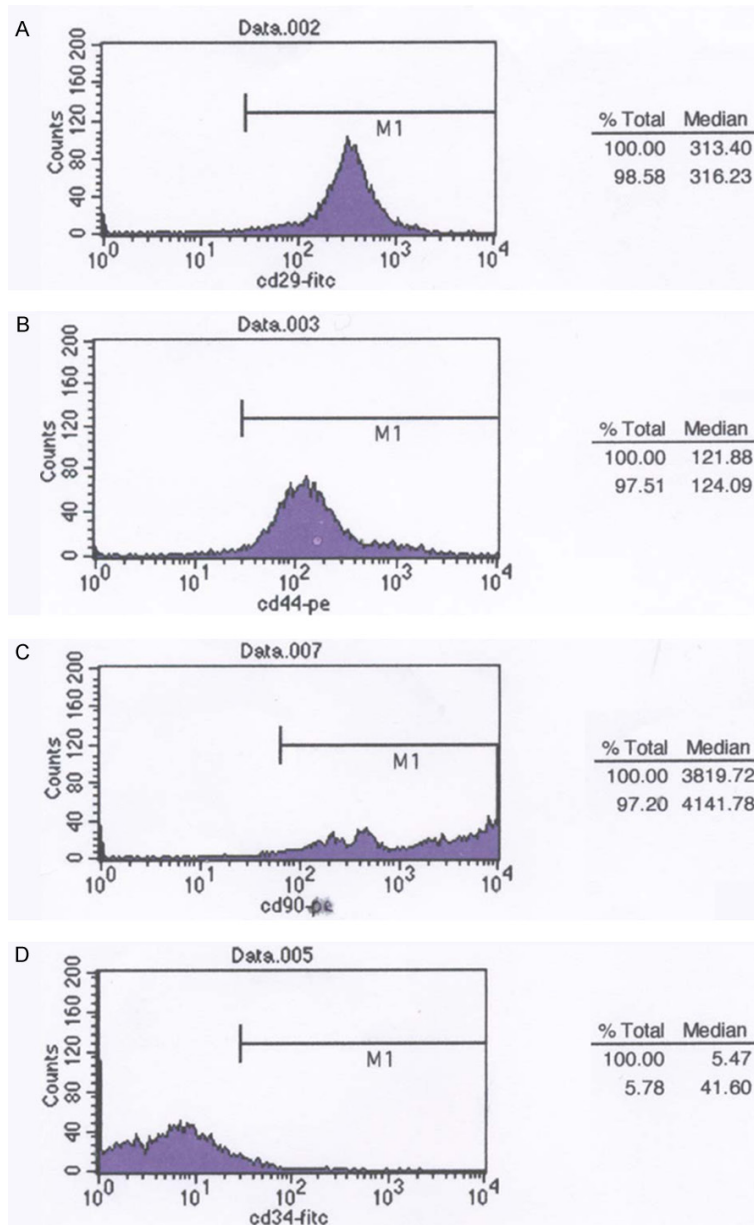


**Figure 2.** Detection of surface antigens of BMSCs in rats at the third passage with flow cytometry. A. CD29 in BMSCs. B. CD44 in BMSCs. C. CD90 in BMSCs. D. CD34 in BMSCs. BMSCs, Bone Marrow Mesenchymal Stem Cells.

## Morphological characteristics of rat BMSCs on nHA/BC copositive scaffolds

Inverted phase contrast microscope was used to observe the characteristics of rat BMSCs on nHA/BC copositive scaffolds. BMSCs were adhered to nHA/BC copositive scaffolds after 24 h culture and presented as circle and short fusiform (Figure 3A). At days 3, most of BMSCs were long fusiform and the gap of cells became smaller (Figure 3B). BMSCs were fused and fully covered nHA/BC scaffolds, and connected

with the cells around nHA/BC scaffolds at 7 days (Figure 3C). BMSCs were fused and grown to one layer on nHA/BC scaffolds at 9 days (Figure 3D).

## Proliferation of rat BMSCs on nHA/BC copositive scaffolds

The proliferation of rat BMSCs on nHA/BC copositive scaffolds was assessed at time points of 1, 3, 5, 7, and 9 d. BMSCs in two groups exhibited a logarithmic multiplication period from 3 to 7 days and displayed a growth inhibition at day 9. The BMSCs on nHA/BC copositive scaffolds proliferated faster than the control group after the 3th day (Figure 4). These results indicated the nHA/BC scaffolds had a good cell biocompatibility, and may be able to promote proliferation of BMSCs.

## Phosphorylated p38 level in BMSCs of different groups

BMSCs were planted on nHA/BC scaffolds and cultured by osteogenic induction medium (Group A); BMSCs were cultured by osteogenic induction medium (Group B); BMSCs were planted on nHA/BC scaffolds and cultured by DMEM-F12 medium (Group C); BMSCs were cultured by DMEM-F12 medium (Group D). Our results showed that the expression of total p38 protein had no significant difference in all groups.

The p38 phosphorylation levels in group A and group B were higher than those in both group C and group D. Moreover, the level of phosphorylated p38 was higher in group A than group B, while the p38 phosphorylation level group C was higher than group D (Figure 5).

## Osteogenic differentiation of BMSCs in different groups

The osteogenic differentiation of BMSCs was evaluated by Alizarin Red staining. Positive

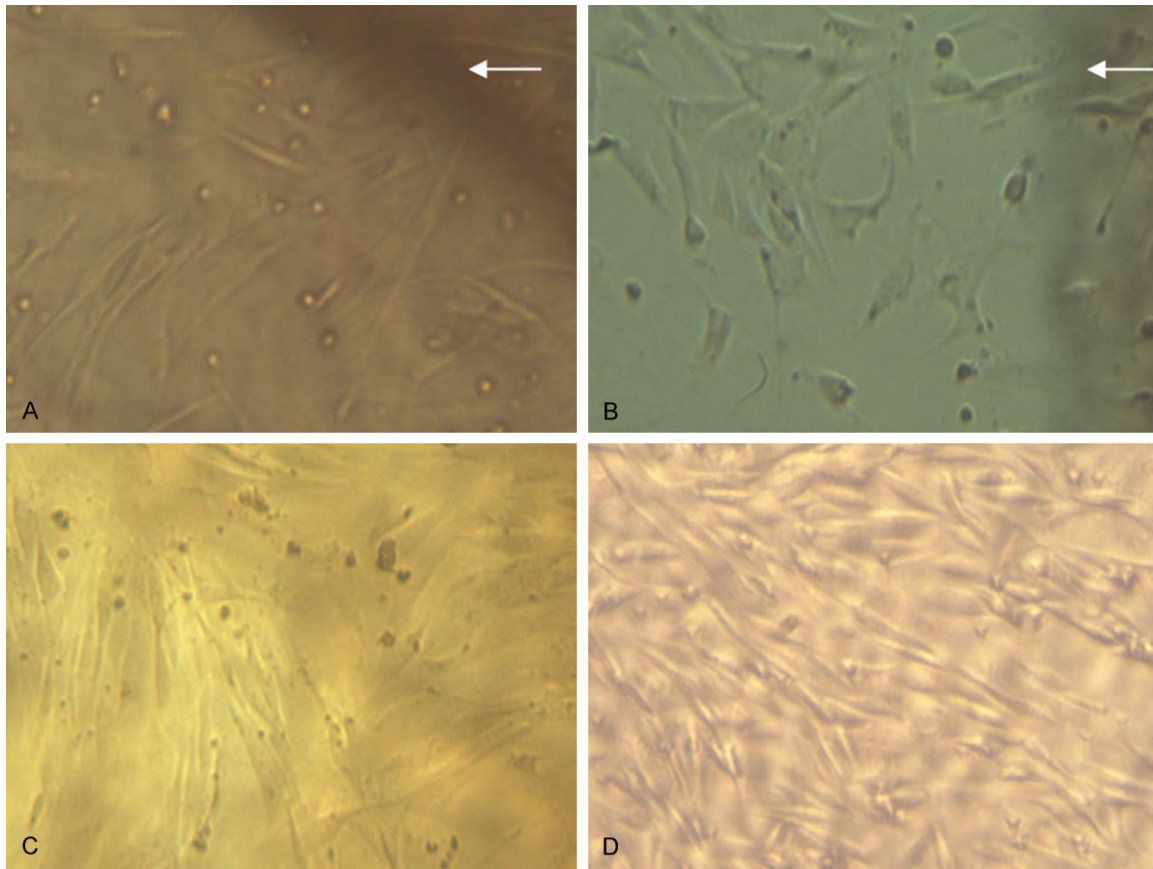


**Figure 3.** Morphological characteristics of BMSCs in rats on nHA/BC coposite scaffold. A. BMSCs on nHA/BC coposite scaffold after 24 h. B. BMSCs on nHA/BC coposite scaffold after 3 days. C. BMSCs on nHA/BC coposite scaffold after 7 days. D. BMSCs on nHA/BC coposite scaffold after 9 days. The arrow indicated the boundary of nHA/BC stent. BMSCs, Bone Marrow Mesenchymal Stem Cells.

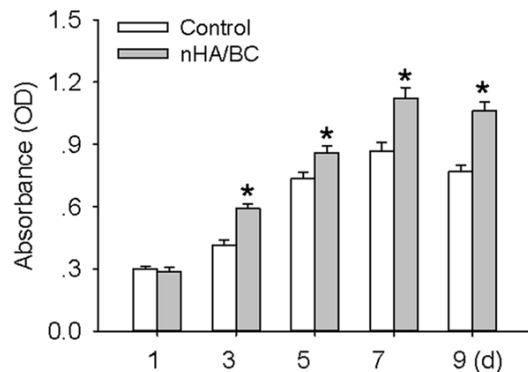


**Figure 4.** The proliferation of rat BMSCs on nHA/BC coposite scaffold evaluated with CCK-8 kits at the indicated time. Values are mean  $\pm$  SD. \* $P < 0.05$  vs. Control.  $n = 6$  for each group. The data in absorbance between groups at the same indicated time were compared with Student's  $t$  test.

Alizarin Red staining through the matrix at the surface layer of group A was greater than that

of the group B. The Alizarin Red staining was negative in group C and group D (**Figure 6**).

## *Osteogenesis in rat muscle pouch observed by CT scanning*

The oval bone development of 1.0 cm $\times$ 1.0 cm $\times$ 0.3 cm appeared on the left muscle pouch (**Figure 7A-C**), while the non-induced group and control group had no bone development.

## *Bone formation of tissues in different groups*

There was no new bone formation on the implanted materials in control group and non-induced group, the nHA/BC scaffolds in both control group and non-induced group was wrapped by thin fiber, the surface of tissues was darker than original materials (**Figure 8A, 8B**). The recombination nHA/BC scaffolds with BMSCs by osteogenic induction was entirely wrapped by white bone tissue with unclear boundary (**Figure 8C**).

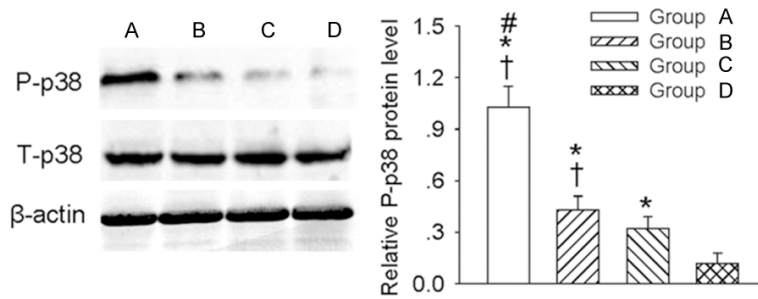


**Figure 5.** The phosphorylated p38 level in BMSCs of different groups. BMSCs were planted on nHA/BC support and cultured by osteogenic induction medium (A); BMSCs were cultured by osteogenic induction medium (B); BMSCs were planted on nHA/BC support and cultured by DMEM-F12 medium (C); BMSCs were cultured by DMEM-F12 medium (D). Values are mean ± SD. \* $P < 0.05$  vs. Group A; † $P < 0.05$  vs Group B; # $P < 0.05$  vs Group C.  $n = 4$  for each group. One-way ANOVA was used to compare the differences in phosphorylated p38 level in different groups, and the comparisons between two groups were analyzed by One-way ANOVA post hoc Bonferroni test.

#### H&E staining for tissues in different groups

It is evidenced that more fibrous tissue, but no bone or cartilage tissue in the pore spaces of implanted nHA/BC scaffolds was present in the control group and non-induced group (Figure 9A, 9B). The mature woven bone and bone trabecular were appeared in the group of BMSCs on nHA/BC scaffolds by osteogenic induction (Figure 9C).

#### Discussion

The reconstructive surgery requiring bone grafts is increasing in worldwide hospitals [27]. Autologous or allogenic bone graft is clinically used for bone repair in bone fractures and trauma-related injuries. However, it is recently reviewed the high risk of disease transmission and rejection in allografts and xenografts [28]. Bone tissue engineering is recognized as an alternative and developing option that has been introduced to improve the osteogenesis of the bone fractures and defects [29]. In the present study, we prepared nHA/BC scaffolds utilizing the biomimetic technique. Our results showed that (1) BMSCs could adhere and spread on nHA/BC scaffolds; (2) BMSCs proliferated faster on the nHA/BC scaffolds than pure BMSCs; (3) osteogenic differentiation of BMSCs on nHA/BC scaffolds was higher than those cultured upon the pure nHA/BC scaffolds in the presence or absence of osteogenic supplements; (4) the new bone formation, mature woven bone and bone trabecular in the pores of the

scaffolds were appeared in BMSCs on nHA/BC scaffolds by osteogenic induction; (5) the nHA/BC scaffolds gradually degraded with bone formation. These results indicated that the attachment, proliferation, and differentiation of BMSCs can be modulated by the nHA/BC scaffolds. We developed a combined nHA/BC scaffolds that exerted a biocompatibility of BMSCs, which may be clinically useful for bone tissue engineering.

Bone tissue engineering is used to develop tissue-engineered constructs that holds osteogenic, osteoinductive

and osteoconductive properties for bone regeneration [14]. The appropriate bioactivity materials for bone tissue engineering include a variety of factors: (1) the scaffolds can be able to regulate the adhesion, growth and differentiation of stem cells; (2) stem cells on scaffolds can undergo differentiation to osteoblasts; (3) the bioresorbable scaffolds can stimulate the cellular attachment, proliferation and differentiation [15]. Moreover, the combined use of scaffolds and BMSCs may open new insights of bone regenerative medicine [6]. The scaffolds of nHA have a good biocompatibility of BMSCs and display a good potential to support the proliferation and osteogenic differentiation of BMSCs [27]. BC has attracted extensive attention all over the world due to its potential as nanofiber scaffolds for bone tissue engineering [20]. In the present study, our results showed that the primary BMSCs were expanded until passage 2, and BMSCs at the second passage were grown to totally confluence with uniform morphology under inverted phase contrast microscope, which are typical morphologic features of BMSCs. In addition, the BMSCs were CD29, CD44, CD90 positive, but CD34 negative, which further confirmed the characters of BMSCs. We also found that BMSCs were adhered to nHA/BC composite scaffolds and fully grown to one layer on nHA/BC scaffolds at 9 days. The BMSCs on nHA/BC composite scaffolds proliferated faster than the control group after the 3th day. These results indicated the nHA/BC scaffolds had a good cell biocompatibility of BMSCs, and may be able to promote proliferation of BMSCs.



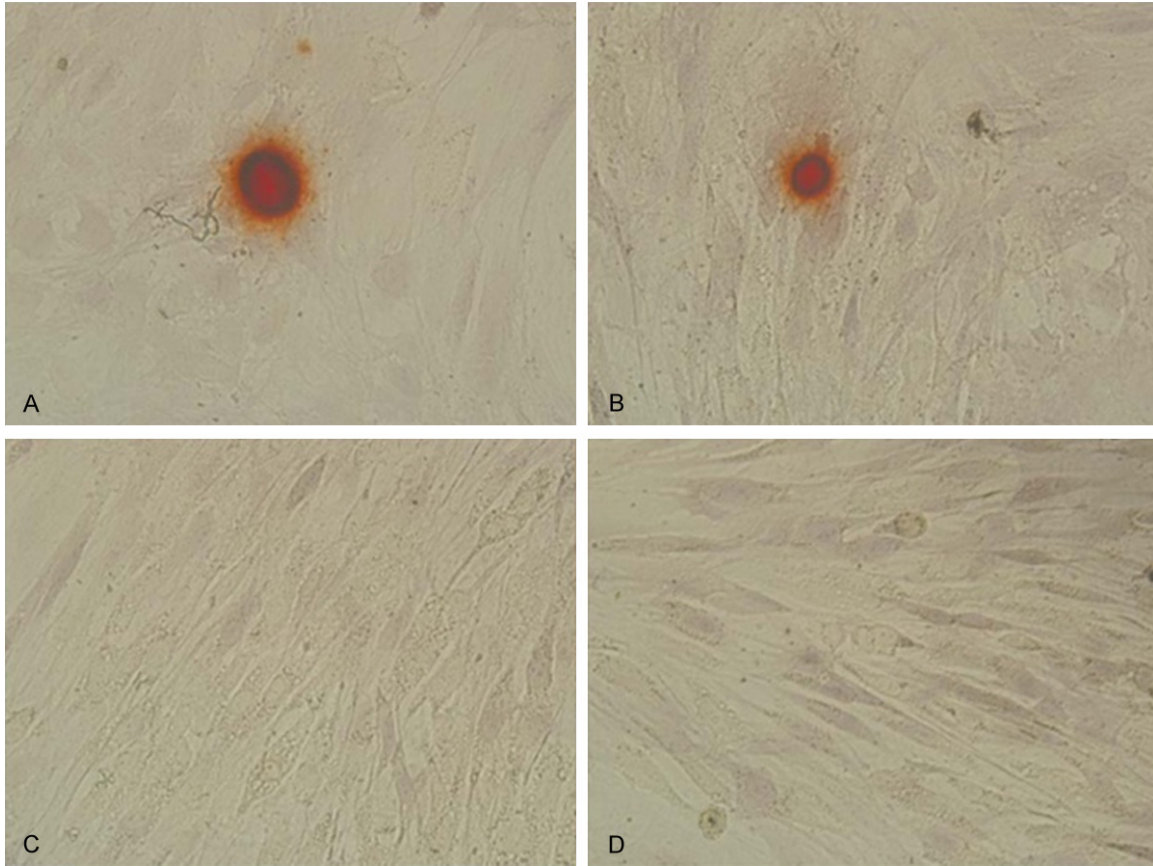


**Figure 6.** Osteogenic differentiation of BMSCs were observed with alizarin red staining in different groups. BMSCs were planted on nHA/BC support and cultured by osteogenic induction medium (A); BMSCs were cultured by osteogenic induction medium (B); BMSCs were planted on nHA/BC support and cultured by DMEM-F12 medium (C); BMSCs were cultured by DMEM-F12 medium (D).

Previous studies disclosed that combined scaffolds-BMSCs may have a better potential in inducing osteogenic differentiation *in vitro* and *in vivo* settings [30]. BMSCs with osteogenic differentiation have been described to be a potential candidate for bone regeneration [31].

It is reported that nHA-chitosan nanocomposites can accelerate the adhesion, proliferation of BMSCs via activation of the integrin-BMP/Smad signaling pathway [32]. The p38-MAPK is critical for osteogenesis and differentiation of BMSCs [33]. Recent study indicates that akermanite bioceramics promote osteogenesis for osteoporotic bone regeneration by activation of p38 signaling pathway [34]. In the present study, we found that BMSCs on nHA/BC scaffolds cultured by osteogenic induction medium significantly promote deposition of calcified matrix on the surface of the culture dish evidenced by alizarin red staining, and stimulated the phos-

phorylation of p38. These results hinted that nHA/BC scaffolds can promote osteogenesis and differentiation of BMSCs associated with p38 activation *in vitro*.

It is revealed that more de novo bone and collagen formation in the pores of the scaffolds gradually increased from 2 weeks post-implantation in group of nHA-chitosan osteo-induced BMSC composites [35]. The scaffolds of calcium phosphate, bone morphogenetic proteins and mesenchymal stem cells can more effectively repair bone defects than an autograft *in vivo* [36]. It is reported that the BMP-VEGF-PLGA-CPC scaffolds have osteogenic and angiogenic activity by radiographic and histological analysis [37]. In present study, we showed that the oval bone development of 1.0 cm×1.0 cm×0.3 cm appeared on the left muscle pouch, the recombination nHA/BC scaffold with BMSCs by osteogenic induction was entirely wra-



## Osteogenesis of bone marrow mesenchymal stem cells



**Figure 7.** Osteogenesis in rat muscle pouch observed by CT scanning. A. The overall figure of rats. B. Location map of Implants osteogenic tissue. C. Bone tissue in muscle pouch of rats subjected to implantation of BMSCs on nHA/BC coposite scaffold by osteogenic induction. The arrow indicated the bone tissue.



**Figure 8.** Bone formation of tissues in different groups. A. The rats were implanted with nHA/BC coposite scaffold without any treatment. B. The rats were implanted with BMSCs on nHA/BC coposite scaffold by ordinary culture medium. C. The rats were implanted with BMSCs on nHA/BC coposite scaffold by osteogenic induction.

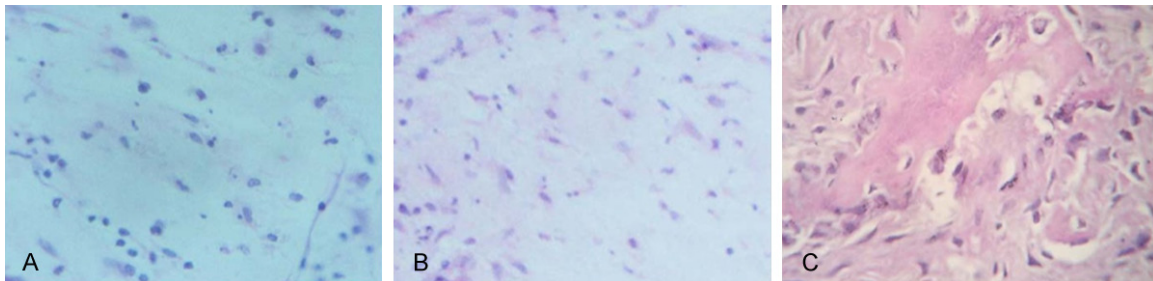


**Figure 9.** HE staining for tissues in different groups. A. The rats were implanted with nHA/BC coposite scaffold without any treatment. B. The rats were implanted with BMSCs on nHA/BC coposite scaffold by ordinary culture medium. C. The rats were implanted with BMSCs on nHA/BC coposite scaffold by osteogenic induction.

pped by white bone tissue with unclear boundary, and the mature woven bone and bone trabecular were appeared in the group of BMSCs on nHA/BC scaffolds by osteogenic induction. These results suggested that nHA/BC osteo-induced BMSC composites significantly enhanced the osteogenic ability and bone formation *in vivo*.

In conclusion, the scaffolds of nHA/BC presented a potential to induce the BMSCs proliferation and ostogenic differentiation via modulation of p38 signal transduction pathway. The

newly developed nHA/BC scaffolds may be considered as a good candidate for bone tissue engineering and bone regenerative medicine applications.

### Acknowledgements

We generously thank public experimental platform of the Affiliated Hospital of Xuzhou Medical University.

### Disclosure of conflict of interest

None.

**Address correspondence to:** Feng Yuan, Department of Spinal Surgery, The Affiliated Hospital of Xuzhou Medical University, 99 Huaihai Road West, Xuzhou 221000, Jiangsu, China. Tel: +86-0516-85609999; Fax: +86-0516-85609999; E-mail: yuanfengxuzhou@sina.com

## References

- [1] Meyer U, Neunzehn J and Wiesmann HP. Computer-aided approach for customized cell-based defect reconstruction. *Methods Mol Biol* 2012; 868: 27-43.
- [2] Ryu TK, Oh MJ, Moon SK, Paik DH, Kim SE, Park JH and Choi SW. Uniform tricalcium phosphate beads with an open porous structure for tissue engineering. *Colloids Surf B Biointerfaces* 2013; 112: 368-373.
- [3] Oe K, Miwa M, Nagamune K, Sakai Y, Lee SY, Niikura T, Iwakura T, Hasegawa T, Shibamura N, Hata Y, Kuroda R and Kurosaka M. Non-destructive evaluation of cell numbers in bone marrow stromal cell/beta-tricalcium phosphate composites using ultrasound. *Tissue Eng Part C Methods* 2010; 16: 347-353.
- [4] Meyer U, Buchter A, Hohoff A, Stoffels E, Szuwart T, Runte C, Dirksen D and Wiesmann HP. Image-based extracorporeal tissue engineering of individualized bone constructs. *Int J Oral Maxillofac Implants* 2005; 20: 882-890.
- [5] Li Q, Wang T, Zhang GF, Yu X, Zhang J, Zhou G and Tang ZH. A Comparative Evaluation of the Mechanical Properties of Two Calcium Phosphate/Collagen Composite Materials and Their Osteogenic Effects on Adipose-Derived Stem Cells. *Stem Cells Int* 2016; 2016: 6409546.
- [6] Elango J, Zhang J, Bao B, Palaniyandi K, Wang S, Wenhui W and Robinson JS. Rheological, biocompatibility and osteogenesis assessment of fish collagen scaffold for bone tissue engineering. *Int J Biol Macromol* 2016; 91: 51-9.
- [7] Amjadian S, Seyedjafari E, Zeynali B and Shabani I. The synergistic effect of nano-hydroxyapatite and dexamethasone in the fibrous delivery system of gelatin and poly(l-lactide) on the osteogenesis of mesenchymal stem cells. *Int J Pharm* 2016; 507: 1-11.
- [8] Zheng K, Chen Y, Huang W, Lin Y, Kaplan DL and Fan Y. Chemically Functionalized Silk for Human Bone Marrow-Derived Mesenchymal Stem Cells Proliferation and Differentiation. *ACS Appl Mater Interfaces* 2016; 8: 14406-13.
- [9] Yousefi AM, James PF, Akbarzadeh R, Subramanian A, Flavin C and Oudadesse H. Prospect of Stem Cells in Bone Tissue Engineering: A Review. *Stem Cells Int* 2016; 2016: 6180487.
- [10] Duarte Campos DF, Blaeser A, Buellesbach K, Sen KS, Xun W, Tillmann W and Fischer H. Bioprinting Organotypic Hydrogels with Improved Mesenchymal Stem Cell Remodeling and Mineralization Properties for Bone Tissue Engineering. *Adv Healthc Mater* 2016; 5: 1336-45.
- [11] Wang H, Zhou Y, Chu TW, Li CQ, Wang J, Zhang ZF and Huang B. Distinguishing characteristics of stem cells derived from different anatomical regions of human degenerated intervertebral discs. *Eur Spine J* 2016; 25: 2691-704.
- [12] Salerno A, Oliviero M, Di Maio E, Netti PA, Rofani C, Colosimo A, Guida V, Dallapiccola B, Palma P, Procaccini E, Berardi AC, Velardi F, Teti A and Iannace S. Design of novel three-phase PCL/TZ-HA biomaterials for use in bone regeneration applications. *J Mater Sci Mater Med* 2010; 21: 2569-2581.
- [13] Udehiya RK, Amarpal, Aithal HP, Kinjavdekar P, Pawde AM, Singh R and Taru Sharma G. Comparison of autogenic and allogenic bone marrow derived mesenchymal stem cells for repair of segmental bone defects in rabbits. *Res Vet Sci* 2013; 94: 743-752.
- [14] Zong C, Qian X, Tang Z, Hu Q, Chen J, Gao C, Tang R, Tong X and Wang J. Biocompatibility and bone-repairing effects: comparison between porous poly-lactic-co-glycolic acid and nano-hydroxyapatite/poly(lactic acid) scaffolds. *J Biomed Nanotechnol* 2014; 10: 1091-1104.
- [15] Tamama K, Sen CK and Wells A. Differentiation of bone marrow mesenchymal stem cells into the smooth muscle lineage by blocking ERK/MAPK signaling pathway. *Stem Cells Dev* 2008; 17: 897-908.
- [16] Lukasheva NV and Tolmachev DA. Cellulose Nanofibrils and Mechanism of their Mineralization in Biomimetic Synthesis of Hydroxyapatite/Native Bacterial Cellulose Nanocomposites: Molecular Dynamics Simulations. *Langmuir* 2016; 32: 125-134.
- [17] Fang B, Wan YZ, Tang TT, Gao C and Dai KR. Proliferation and osteoblastic differentiation of human bone marrow stromal cells on hydroxyapatite/bacterial cellulose nanocomposite scaffolds. *Tissue Eng Part A* 2009; 15: 1091-1098.
- [18] Grande CJ, Torres FG, Gomez CM and Bano MC. Nanocomposites of bacterial cellulose/hydroxyapatite for biomedical applications. *Acta Biomater* 2009; 5: 1605-1615.
- [19] Aminizadeh N, Tiraihi T, Mesbah-Namin SA and Taheri T. Stimulation of cell proliferation by glutathione monoethyl ester in aged bone marrow stromal cells is associated with the assistance of TERT gene expression and telomerase activity. *In Vitro Cell Dev Biol Anim* 2016; 52: 772-81.
- [20] Yue W, Yan F, Zhang YL, Liu SL, Hou SP, Mao GC, Liu N and Ji Y. Differentiation of Rat Bone

- Marrow Mesenchymal Stem Cells Into Neuron-Like Cells In Vitro and Co-Cultured with Biological Scaffold as Transplantation Carrier. *Med Sci Monit* 2016; 22: 1766-1772.
- [21] Wang C, Shi D, Song X, Chen Y, Wang L and Zhang X. Calpain inhibitor attenuates ER stress-induced apoptosis in injured spinal cord after bone mesenchymal stem cells transplantation. *Neurochem Int* 2016; 97: 15-25.
- [22] Landim de Barros T, Brito VG, do Amaral CC, Chaves-Neto AH, Campanelli AP and Oliveira SH. Osteogenic markers are reduced in bone-marrow mesenchymal cells and femoral bone of young spontaneously hypertensive rats. *Life Sci* 2016; 146: 174-183.
- [23] Sun HJ, Zhao MX, Ren XS, Liu TY, Chen Q, Li YH, Kang YM, Wang JJ and Zhu GQ. Salusin-beta Promotes Vascular Smooth Muscle Cell Migration and Intimal Hyperplasia After Vascular Injury via ROS/NFkappaB/MMP-9 Pathway. *Antioxid Redox Signal* 2016; 24: 1045-57.
- [24] Sun HJ, Chen D, Han Y, Zhou YB, Wang JJ, Chen Q, Li YH, Gao XY, Kang YM and Zhu GQ. Relaxin in paraventricular nucleus contributes to sympathetic overdrive and hypertension via PI3K-Akt pathway. *Neuropharmacology* 2016; 103: 247-256.
- [25] Gu Y, Zhou J, Wang Q, Fan W and Yin G. Ginsenoside Rg1 promotes osteogenic differentiation of rBMSCs and healing of rat tibial fractures through regulation of GR-dependent BMP-2/SMAD signaling. *Sci Rep* 2016; 6: 25282.
- [26] Ailawadi S, Wang X, Gu H and Fan GC. Pathologic function and therapeutic potential of exosomes in cardiovascular disease. *Biochim Biophys Acta* 2015; 1852: 1-11.
- [27] Allsopp BJ, Hunter-Smith DJ and Rozen WM. Vascularized versus Nonvascularized Bone Grafts: What Is the Evidence? *Clin Orthop Relat Res* 2016; 474: 1319-1327.
- [28] Oryan A, Alidadi S, Moshiri A and Maffulli N. Bone regenerative medicine: classic options, novel strategies, and future directions. *J Orthop Surg Res* 2014; 9: 18.
- [29] Nagasaki R, Mukudai Y, Yoshizawa Y, Nagasaki M, Shiogama S, Suzuki M, Kondo S, Shintani S and Shirota T. A Combination of Low-Intensity Pulsed Ultrasound and Nanohydroxyapatite Concordantly Enhances Osteogenesis of Adipose-Derived Stem Cells From Buccal Fat Pad. *Cell Med* 2015; 7: 123-131.
- [30] Wu L, Zhao X, He B, Jiang J, Xie XJ and Liu L. The Possible Roles of Biological Bone Constructed with Peripheral Blood Derived EPCs and BMSCs in Osteogenesis and Angiogenesis. *Biomed Res Int* 2016; 2016: 8168943.
- [31] Zheng L, Tu Q, Meng S, Zhang L, Yu L, Song J, Hu Y, Sui L, Zhang J, Dard M, Cheng J, Murray D, Lian J, Stein G and Chen J. Runx2/DICER/miRNA Pathway in Regulating Osteogenesis. *J Cell Physiol* 2017; 232: 182-91.
- [32] Liu H, Peng H, Wu Y, Zhang C, Cai Y, Xu G, Li Q, Chen X, Ji J, Zhang Y and OuYang HW. The promotion of bone regeneration by nanofibrous hydroxyapatite/chitosan scaffolds by effects on integrin-BMP/Smad signaling pathway in BMSCs. *Biomaterials* 2013; 34: 4404-4417.
- [33] Zhou Y, Wu Y, Jiang X, Zhang X, Xia L, Lin K and Xu Y. The Effect of Quercetin on the Osteogenic Differentiation and Angiogenic Factor Expression of Bone Marrow-Derived Mesenchymal Stem Cells. *PLoS One* 2015; 10: e0129605.
- [34] Xia L, Yin Z, Mao L, Wang X, Liu J, Jiang X, Zhang Z, Lin K, Chang J and Fang B. Akermanite bioceramics promote osteogenesis, angiogenesis and suppress osteoclastogenesis for osteoporotic bone regeneration. *Sci Rep* 2016; 6: 22005.
- [35] He Y, Dong Y, Cui F, Chen X and Lin R. Ectopic osteogenesis and scaffold biodegradation of nano-hydroxyapatite-chitosan in a rat model. *PLoS One* 2015; 10: e0135366.
- [36] Sun H and Yang HL. Calcium phosphate scaffolds combined with bone morphogenetic proteins or mesenchymal stem cells in bone tissue engineering. *Chin Med J (Engl)* 2015; 128: 1121-1127.
- [37] Zhang HX, Zhang XP, Xiao GY, Hou Y, Cheng L, Si M, Wang SS, Li YH and Nie L. In vitro and in vivo evaluation of calcium phosphate composite scaffolds containing BMP-VEGF loaded PLGA microspheres for the treatment of avascular necrosis of the femoral head. *Mater Sci Eng C Mater Biol Appl* 2016; 60: 298-307.